Full Paper

Wiley Online Library

ELECTROANALYSIS

DOI: 10.1002/elan.201700612

A Biosensor for Genetic Modified Soybean DNA Determination via Adsorption of Anthraquinone-2-sulphonic Acid in Reduced Graphene Oxide

Raja Zaidatul Akhmar Raja Jamaluddin,[a] Lee Yook Heng,*[a, b] Ling Ling Tan,[b] and Kwok Feng Chong*[c]

Abstract: An electrochemical DNA biosensor for DNA determination of genetically modified (GM) soybean (CaMV 35S target genes) was developed utilizing a new detection concept based on the adsoption of anthraquinone-2-sulphonic acid (AQMS) on the reduced graphene oxide nano-particles (rGO) during DNA hybridization events. The aminated DNA probe for CaMV 35S was immobilized onto poly(*n*-butyl acrylate) film modified with succinimide functional groups [poly(*n*BA-NAS)] via peptide covalent bond. Nanosheets of rGO were entrapped in the poly(*n*BA-NAS) film to form a conducting [poly(*n*BA-NAS)-rGO] film of the DNA biosensor. Besides facilitating the electron transfer reactions, the rGO also functioned as an adsorbent for AQMS. The sensing mechanism of the proposed DNA biosensor involved measuring the oxidation current of the AQMS adsorbed on the electrode surface at −0.50 V using differential pulse voltammetry (DPV) before and after a DNA hybridization event. Under optimum conditions, the DNA biosensor demonstrated a linear proportionality between AQMS oxidation signal and logarithm cDNA concentration from 1.0×10^{-15} M to 1.0×10^{-8} M target DNA with a detection limit of 6.3×10^{-16} M. The electrochemical DNA biosensor possessed good selectivity and a shelf life of about 40 days with relative standard deviation of reproducibility obtained in the range of 3.7–4.6% ($n=5$). Evaluation of the DNA biosensor using GM soybean DNA extracts showed excellent recovery percentages of 97.2–104.0.

Keywords: AQMS · DPV · GMO biosensor · Graphene · Poly(*n*-butyl acrylate)

1 Introduction

Electrochemical DNA biosensor based on sequence specific hybridization detection generally involves the reduction of purine bases i.e. guanine and adenine. Therefore, sequence specific information can be acquired as a function of current, potential, conductivity, impedance and capacitance [1] through several electrochemical methods such as differential pulse voltammetry (DPV), square wave voltammetry (SWV) and potentiometric stripping analysis (PSA) [2]. Direct electrochemical detection of DNA offers the covenience of label-free detection but delivers a sensitivity that is far inferior than label-based DNA assays [3,4]. To overcome this limitation, DNA hybridization reaction on a biosensor can be determined by using a mediator. Palecek et al. [5] suggested the addition of a redox active material would assist in the amplification of signal and sensitivity of the DNA biosensor, which could be seen in many previously reported studies applying various electroactive intercalators in the investigation of DNA hybridization reaction [6,7,8,9]. It has been claimed that the use of anionic anthraquinone compound as a redox intercalator can effectively eliminate the background electrochemical signals and improve the overall DNA biosensor sensitivity performance [7], but the main drawback is that a prolonged incubation period is required for the intercalation activity to take place owing to the same charge of both double-stranded DNA (dsDNA) and anthraquinone intercalative agent, which impedes the rapid DNA detection [10,11]. Apart from anthraquinone derivatives, other organic compounds and aromatic species, which are

[a] R. Z. A. R. Jamaluddin, L. Y. Heng
School of chemical Sciences and Food Technology, Faculty of Science & Technology, Universiti Kebangsaan Malaysia, 43600 UKM Bangi, Selangor Darul Ehsan, Malaysia
E-mail: anne2282@yahoo.com
leeyookheng@yahoo.co.uk

[b] L. Y. Heng, L. L. Tan
Southeast Asia Disaster Prevention Research Initiative (SEADPRI-UKM), <orgDiv/Institute for Environment and Development (LESTARI), Universiti Kebangsaan Malaysia, 43600 UKM Bangi, Selangor Darul Ehsan, Malaysia
E-mail: babybaeoo@gmail.com

[c] K. F. Chong
Faculty of Industrial Sciences & Technology, Universiti Malaysia Pahang, Lebuhraya Tun Razak, 26300 Gambang, Kuantan, Pahang Darul Makmur, Malaysia
E-mail: ckfeng@ump.edu.my

Supporting information for this article is available on the WWW under https://doi.org/10.1002/slct.201700612

rich in π orbitals were identified to be easily adsorbed onto aromatic macromolecules such as graphite surfaces, graphene and carbon nanotube (CNT) through π-π staking interaction. The nature of the interaction effect may be one of the reasons why carbon-based materials and their derivatives are normally used in limited amounts in electrochemical detection of aromatic analytes.

Because of the π-π staking interaction between anthraquinone derivatives and graphene materials, a large unspecific current can be produced if anthraquinone derivatives is used as a DNA intercalator in a DNA biosensor that contains graphene as a membrane material. This leads to loss of specificity of the DNA determination. However, such adsorption behaviour of anthraquinone derivatives onto graphene can also be exploited for DNA determination based on the concept of blocking by hybridized DNA on anthraquinone derivatives adsorption on a surface. In this work, we explored the possibility of utilizing anthraquinone-2-sulphonic acid (AQMS) adsorption onto graphene materials as an indication of DNA hybridization to construct a biosensor for DNA determination. The biosensor was built based on succinimide-functionalized poly(n-butyl acrylate) membrane containing embedded graphene (rGO) nanosheets deposited on a carbon paste screen-printed electrode (SPE). Aminated DNA probe was immobilized onto the poly(n-butyl acrylate-co-N-acryloxysuccinimide) membrane containing graphene [poly(nBA-NAS)-rGO] by covalent coupling via amide bond. With this electrode design, the effect of hybridization on the adsorption behaviour of AQMS redox indicator onto the rGO in the composite can be studied.

The DNA biosensor created based on such concept was also utillized to determine the presence of modified gene in soybean where the detection and identification of genetically modified (GM) food intakes for consumers are of current concern. Electrochemical DNA biosensor provides an alternative method for simpler yet rapid assay of GM DNA in food compared to conventional molecular biology techniques. The DNA biosensor for the analysis of GM soybean was based on monitoring of the oxidation peak current of the adsorbed AQMS on the poly(nBA-NAS) polymer. The detection was performed by differential pulse voltammetry (DPV). The schematic design and the working principle of the electrochemical DNA biosensor is illustrated in Figure 1.

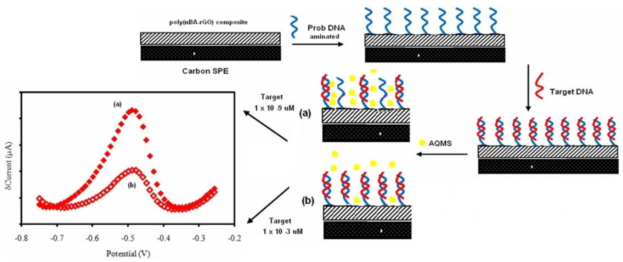

Fig. 1. The schematic design and principle of operation of the electrochemical GM DNA biosensor based on poly(nBA-NAS)-rGO modified SPE.

2 Experimental

2.1 Instrumentation

Surface morphology of the reduced graphene oxide (rGO) was studied by field emission scanning electron microscopy (FESEM, JEOL JSM-7800F) at an acceleration voltage of 3.0 kV and 160 k × magnification. Raman spectrum of the graphene nanomaterials was examined by using Renishaw (In-Via) Raman microscope with the 532 nm excitation laser source. Cyclic Volatammetry (CV) and DPV measurements were performed with Autolab PGSTAT 12 (Metrohm) potentiostat. Carbon paste screen printed electrode (SPE) modified with poly(*n*BA-NAS)-rGO composite film was used as the working electrode. Carbon pencil and Ag/AgCl electrodes were used as auxiliary and reference electrodes, respectively. All the potentials measured in this study were referred to Ag/AgCl electrode in 0.05 M sodium phosphate (Na-phosphate) electrolyte buffer (pH 7.0). Homogeneous solutions were prepared using Elma S30H sonicator bath.

2.2 Chemicals and Reagents

Na-phosphate buffer at 0.05 M and pH 7.0 was prepared by mixing an appropriate amount of 0.05 M disodium hydrogen phosphate (Na_2HPO_4) with 0.05 M sodium dihydrogen phosphate (NaH_2PO_4). Anthraquinone monosulfonic acid (AQMS, Acro organics) solution (1 mM) was prepared by dissolving AQMS in 0.05 M Na-phosphate buffer (pH 7.0). Aldrich supplied n-butyl acrylate (*n*BA), 2-2-dimethoxy-2-phenylacetophenone (DMPP) and 1,6-hexanadiol diacrylate (HDDA). N-acryloxysuccinimide (NAS) was sourced from Across, whilst potassium ferricyanide ($K_3[Fe(CN)_6]$) was obtained from Merck. Complementary DNA of CaMV 35S (cDNA), non-complementary DNA (ncDNA) and mismatch DNA sequences were designed by Malaysian Agricultural Research & Development Institute. DNA probe for immobilization was designed with an additional amine functional group with a C_7 linker. Table S1 in Supporting Information lists the 20-base synthetic oligonucleotides (Sigma-Aldrich, 100 μM) that were used in this study. GM soybean was purchased from Roundup Ready GM-soybean (Monsanto, USA) with 0% and 5% (w/w) (20 μg/mL) GM contents. GM soybean standards were obtained from Fluka Chemical Co. (Switzerland). Stock solution of DNA probe for immobilization was diluted with 0.05 M Na-phosphate buffer at pH 7.0, whilst other DNA stocks were diluted with 0.05 M Na-phosphate buffer (pH 6.5) containing 0.5 M sodium chloride (NaCl, Systerm). All the aqueous solutions were prepared using deionized water.

2.3 Synthesis of Graphene Oxide and Graphene Nanosheets

Graphene oxide (GO) was prepared from graphite powders based on Hummers and Offeman [12] method. Prior to GO synthesis, an additional graphite oxidation procedure was conducted according to the recommendation provided by Kovtyukhova et al [13] otherwise incomplete oxidized graphite-core/GO-shell particles will be observed in the final product. The precursor of GO was first dispersed in water followed by the addition of KOH solution (Figure 2). According to Park and Ruoff [14], KOH, a strong base, can confer a large negative charge through reactions with the reactive hydroxyl, epoxy and carboxylic acid groups on the GO sheets, resulting in extensive coating of the sheets with negative charges and K^+ ions. The addition of 0.25 mL hydrazine monohydrate (100 mmol) to KOH-treated GO later produced a homogeneous suspension, which can remain stable for at least 4 months. The as-produced GO suspension was then ultrasonicated to form a clear solution without any visible particulate matters [15] and heated in an oil bath at about 95 °C for 24 h. As a result, the as-synthesized rGO (reduced graphene oxide) gradually precipitated as a black solid. Finally, it was filtered and washed with copious volumes of deionized water (500 mL) and acetone (500 mL), and dried overnight in a vacuum desiccator.

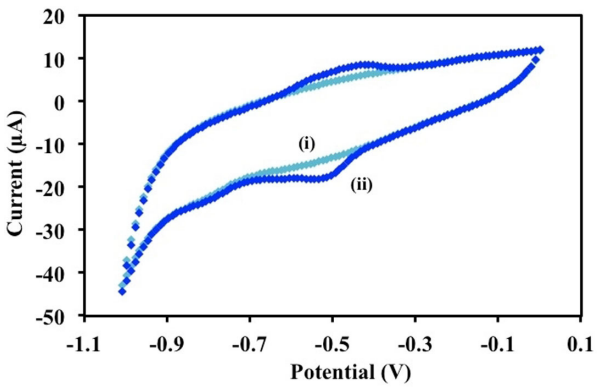

Fig. 2. The cyclic voltammograms of poly(*n*BA-NAS)-rGO modified SPE (i) before and (ii) after exposure to 1 mM AQMS solution for 1 h.

2.4 Preparation of Poly(*n*BA-NAS)-rGO Composite Membrane and DNA Electrode

The photocuring mixture for poly(nBA-NAS) was prepared by mixing 950 µL of *n*BA monomer with 3 µL of HDDA crosslinking agent and 3 mg of NAS. About 1 mg of rGO was dissolved in 200 µL of dimethylformamide (DMF, Sigma-Aldrich), and subsequently added into 125 µL of photocuring mixture solution in the presence of 2 mg DMPP, and sonicated to obtain a uniform solution. A total of 5 µL of this mixture was then drop-casted onto the SPE, and exposed to UV radiation for 180 s under nitrogen gas atmosphere to initiate the photopolymerization reaction at the SPE surface, and thus forming the poly(*n*BA-NAS)-rGO composite membrane. The poly(-*n*BA-NAS)-rGO modified SPE was immersed overnight in 300 µL of 5 µM aminated DNA probe solution at pH 7.0 for covalent coupling of DNA probes on the poly(*n*BA-NAS) membrane coated on the SPE surface. The DNA probe-immobilized poly(*n*BA-NAS)-rGO modified SPE was finally washed with abundant deionized water to remove non-specific adsorbed DNA probes on the rGO-modified acrylic film electrode.

2.5 Evaluation of Biosensor Response

The response of AQMS on the poly(*n*BA-NAS)-rGO modified SPE was studied with CV between the potential window of −1.1 V and 0.1 V at a scan rate of 0.1 V/s to establish its interaction behavior with the graphene.

For the DNA biosensor response, it was evaluated by measuring the hybridization to cDNA strand via soaking the DNA electrode into 5 µM of cDNA solution in 0.05 M Na-phosphate buffer (pH 6.5) containing 0.5 M NaCl for one and a half hours followed by immersion of the DNA biosensor in 1 mM AQMS solution for another 1 h at room temperature (25 °C). The electrochemical response of the DNA biosensor was later measured with DPV method in 0.05 M Na-phosphate buffer (pH 7.0) at a peak current at −0.5 V. The adsorption of the AQMS on the electrode without undergo any DNA hybridization reaction was also determined at −0.5 V using an electrode fabricated from the same batch.

Optimum AQMS accumulation time on the DNA biosensor was determined by measuring the AQMS DPV peak current at −0.5 V between 1 h and 24 h. The effect of rGO loading in the poly(*n*BA-NAS) matrix on the DNA biosensor response was carried out by varying the volume ratio of rGO solution (in DMF) to photocuring mixture from 1.0:0.1 to 1.0:1.0. DNA probe concentration effect study was performed by changing the DNA probe loading on the poly(*n*BA-NAS)-rGO composite SPE between 1 µM and 5 µM, whilst the cDNA concentration was remained constant at 5 µM. The effects of pH, Na^+ ion and buffer concentrations were assessed by varying the Na-phosphate buffer pH from pH 6–8, NaCl concentration from 0.1–2.0 M and Na-phosphate buffer capacity from 0.01–0.5 M. For the determination of optimum DNA probe immobilization time, the poly(*n*BA-NAS)-rGO modified SPE was immersed in 5 µM DNA probe solution from 1–24 h. Next, the optimum DNA hybridization time was studied by immersing the DNA electrode into 5 µM cDNA solution from 30–180 min. The lifetime of the DNA biosensor for determination of targeted DNA was investigated by using 33 DNA biosensors, which were kept at 4 °C in a refrigerator. The amperometric signal of these DNA biosensors towards the detection of 1.0×10^{-9} µM cDNA at −0.5 V was then measured at different

days over a four-month period. The linear dynamic response range of the DNA biosensor was examined with different cDNA concentrations from 1.0×10^{-11}–1.0×10^{-2} μM, and the DPV response was taken 90 min after the DNA hybridization reaction completed. To assess the selectivity of the DNA biosensor, the DNA electrode was exposed to non-complementary mismatch DNA sequences at the concentrations of 5 μM and 0.5 μM, and compared the DNA biosensor response with cDNA as well as a blank electrode without immobilized DNA probe. The reproducibility of the DNA biosensor response was evaluated by using five DNA electrodes for detection of target DNA concentrations at 1.0×10^{-5} μM and 1.0×10^{-8} μM.

2.6 Evaluation of DNA Biosensor for Real GM Soybean DNA Extract Analysis

The accuracy and feasibility of the DNA biosensor from this study for GM food testing was examined by using DNA extracts of standard GM soybean (20 μg/mL) from Monsanto USA, which contained known amount of GM content (obtained from Malaysian Agricultural Research & Development Institute). The GM soybean DNA extracts were diluted with 0.05 M Na-phosphate buffer at pH 6.5 to yield a series of GM DNA concentrations from 2.0×10^{-8}–5.0×10^{-4} μg/mL. The DNA biosensor DPV signal measuremant was carried out after incubation of the DNA electrode into the respective DNA extracts of GM soybean for 90 min.

3 Results and Discussion

3.1 FESEM and Raman Spectroscopic Studies of Reduced Graphene Oxide

The FESEM image in Figure S1(a) from the Supporting Information shows curvy and wrinkled sheets of the assythesized rGO, which was associated with the exfoliation treatment via ultrasonication during the process of graphene synthesis. This expanded morphology is essential in the immobilization process as it maximizes the surface area available for DNA immobilization. As FESEM image signifies, the average thickness of the resulting graphene nanosheets are around 2–4 nm

The Raman spectra of rGO is shown in Supporting Information, Figure S1(b). Raman specstroscopy is useful for studying disorder and defects in crystal structure, particularly in carbon struture. Disorder is determined by the intensity ratio between the disorder induced D band and the Raman allowed G band (ID/IG) [16]. The ID/IG also provides information on the distance between defects in carbon structure [17]. The D band is seen at 1351.7 cm^{-1} and 1348.9 cm^{-1}, and the G band is seen at 1593.7 cm^{-1} and 1586.9 cm^{-1} for GO and rGO, respectively. The G band of GO appears in slightly higher wavenumber as compared to that of rGO, could be attributed to the oxygen functionalization in GO and the increase number of sp^2 domain in rGO. The ID/IG ratio is computed to be 0.90 and 1.04 for GO and rGO, respectively. The higher ratio indicates the removal of oxygen functional groups in GO and creating more defect sites in rGO.

3.2 Investigation on The Effect of DNA Hybridization Towards Absorption Behaviour of AQMS on The DNA Electrode

Anthraquinone derivatives are commonly used as electroactive labels in the electrochemical DNA detection. Besides, it is also feasible to graft anthraquinone directly onto carbon materials via non-covalent interactions between aromatic rings [18]. The redox peaks of AQMS before and after the poly(*n*BA-NAS)-rGO modified SPE exposed to 1 mM AQMS are presented in the cyclic voltammograms in Figure 2. An obvious anodic peak potential of AQMS was observed at −0.5 V after the poly(*n*BA-NAS)-rGO composite electrode exposed to 1 mM AQMS for 1 h as the adsorbed AQMS on the electrode surface oxidized to generate two H^+ ions and two electrons [19,20]. This indicates the AQMS can physically adsorb on the poly(*n*BA-NAS)-rGO composite electrode possibly by non-covalent π-π staking between benzene rings of anthraquinone molecule and hexagonal cells of graphene sheets [7].

The DPV response of the DNA electrode towards 5 μM cDNA detection was examined by first reacting the DNA electrode with 5 μM cDNA in 0.05 M Na-phosphate buffer (pH 6.5) containing 0.5 M NaCl for 90 min followed by immersing the dsDNA electrode in 1 mM AQMS solution for 1–24 h. At the begining where there was no exposure to cDNA (blank response, Figure 3), the DPV current at −0.5 V of the electrode was the highest indicating maximum adsorption of AQMS on the graphene. In the presence of cDNA, the current began to decrease with time and this is attributed to the hybridization of the cDNA with the immobilized DNA probes, which leads to blocking of the adsorption of the AQMS on the graphene. The decrement in current becomes

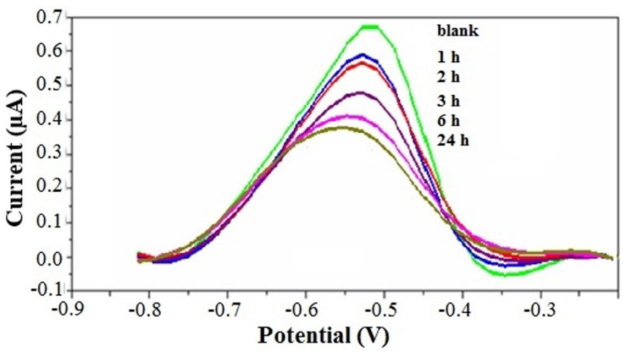

Fig. 3. The DPV response of the DNA biosensor towards 5 μM cDNA at different AQMS intercalation durations from 1–24 h using 1 mM AQMS solution.

larger when the exposure time to cDNA was longer, especially after three hours, indicating more extensive hybridization had occurred. This finding is supported Wong and Gooding [11] where they had encountered a lengthy incubation time for DNA hybridization when using an anionic anthraquinone intercalator in the DNA assay because of charge repulsion. It is also observed in Figure 3 that the DPV peak of AQMS shifted as the exposure time to cDNA was increased indicating intercalation of AQMS and hence hybridization of DNA became dominant over adsorption of graphene after approximately 3 h of exposure to cDNA [21].

The above observation can be further confirmed by studies using electrodes with different membrane compositions that had been exposed to AQMS. Figure 4 demonstrates the DPV responses of AQMS from electrodes with different membrane materials. When the electrodes contained only graphene, highest DPV response was obtained but when the polyacrylic membrane was coated with graphene, slight reduction of AQMS current was observed (Figure 4a and Figure 4b). Thus, both indicated the adsorption ability of AQMS in the absence of immobilized DNA probes. In the presence of 5 μM cDNA, a very obvious reduction in the DPV current of AQMS was observed (Figure 4c). This is attributed to the hybridization of the cDNA with the immobilized DNA probes and hence blocking the electrode surface and restricted the AQMS absorption on the poly(*n*BA-NAS)-rGO electrode membrane. When the DNA electrode was exposed to ncDNA, the response current is much higher than that of cDNA (Figure 4d) and this showed that the electrode could distinguish between complementary and non-completementary DNA strands. However, the current obtained in (d) is lower than that of Figure 4a and Figure 4b because of the presence of immobilized DNA probes on the membrane. This should have exerted some blocking effect on the adsorption of AQMS. The above data has confirmed that the mechanism proposed for DNA determination is indeed can be employed for DNA determination in a DNA biosensor. Thus, further optimization of the DNA biosensor is needed for further application.

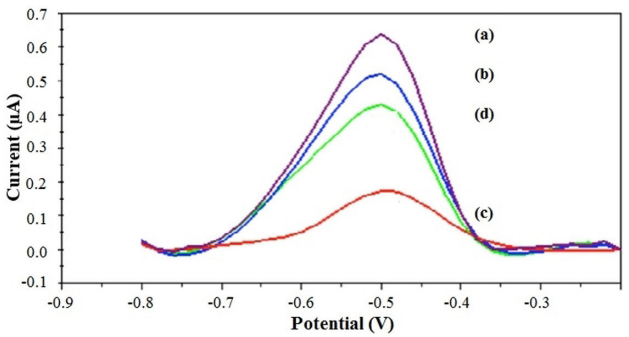

Fig. 4. The differential pulse voltammograms of electrode response to AQMS: (a) Electrode coated with only rGO, (b) Electrode coated with poly(*n*BA-NAS)-rGO, (c) Electrode of DNA-poly(*n*BA-NAS)-rGO after exposure to 5 μM cDNA, (d) Electrode of DNA-poly(*n*BA-NAS)-rGO after exposure to ncDNA. The AQMS solution used is in 0.05 M Na-phosphate buffer (pH 6.5) with exposure time of 1 h.

3.3 Graphene and DNA Probe Loadings on the DNA Biosensor Response

The amount of graphene nanoparticles immobilized in the poly(*n*BA-NAS) membrane is imperative to ensure optimum AQMS adsorption at the composite membrane surface. As presented in Figure S2(a) in Supporting Information, the DNA biosensor response increased proportionally with the increasing of the rGO loading in the sensor membrane from the photocuring mixture to rGO [poly(*n*BA-NAS):rGO] volume ratio of 1.0:0.1 to 1.0:0.7 due to the increment in the amount of non-specific adsorption of AQMS on the DNA-poly(*n*BA-NAS)-rGO composite membrane. This was attributed to the fact that higher loading of rGO in the polyacrylic membrane favoured the π–π stacking between AQMS anthraquinone benzene rings and aromatic carbons in graphene. However, excessive amount of rGO in the polyacrylic membrane at a volume ratio of 1.0:1.0 has hindered the electron transfer to the electrode as the AQMS oxidized at the SPE surface.

In contrast to this, the DNA biosensor response from hybridization with 5 μM cDNA was noticed to decline as the DNA probe loading increased from 1–5 μM [Supporting Information, Figure S2(b)]. This was attributed to the competitive binding of AQMS and DNA probe on the DNA-poly(*n*BA-NAS)-rGO composite membrane. At lower immobilized DNA probe concentrations (i.e. between 1 μM and 3 μM), the surface of the DNA-poly(*n*BA-NAS)-rGO composite membrane was partially occupied, thus promoting adsorption of AQMS on the electrode surface. When 5 μM of DNA probe was immobilized onto the composite membrane, the available binding sites for DNA probe are presumably mostly occupied, thus after hybridization, maximum decrease in DPV current was observed attributed to minimum adsorption of AQMS. Therefore, DNA probe loading was maintained at 5 μM in the subsequent experiments since lowest current response indicated maximum DNA hybridization.

3.4 pH, Ionic Strength and Buffer Capacity Effects on The DNA Biosensor Response

The effect of pH towards the DNA hybridization reaction on the DNA biosensor was demonstrated in Figure 5a. In acidic conditions i.e. below pH 5, the DNA phosphodiester chain was undergoing protonation reaction, and consequently decreasing the solubility of DNA molecules, thereby reducing the DNA hybridization reaction [22]. Between pH 7 and pH 8, AQMS adsorption and oxidation reactions became more dominant, especially towards alkaline pH. This was because the basic buffer solution

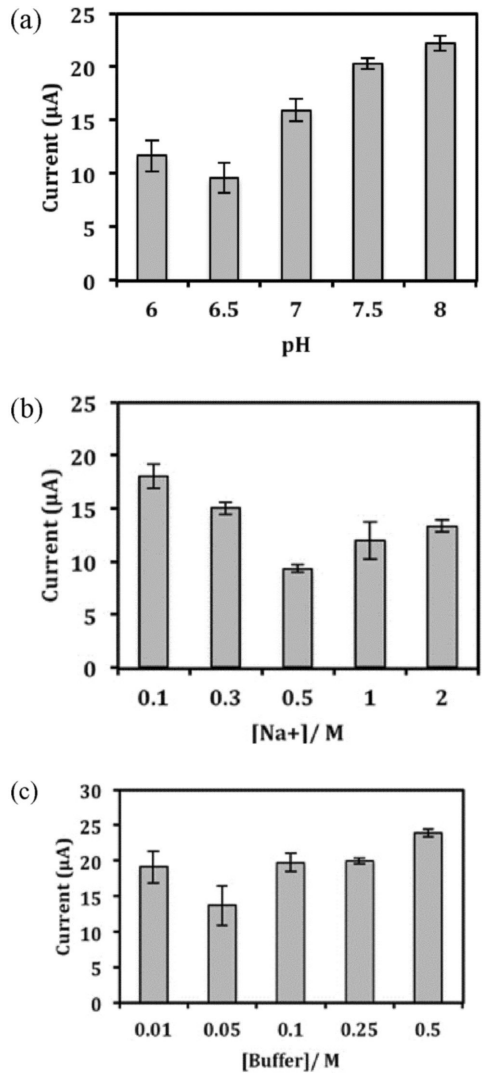

Fig. 5. Effects of pH (a) ionic strength (b) and buffer concentration (c) on the GMO DNA biosensor response upon hybridization with 5 μM cDNA and accumulation with 1 mM AQMS in 0.05 M Na-phosphate buffer (pH 6.5).

has broken up the weak hydrogen bonds between nucleobases, and the immobilized dsDNA helical structure become denatured. Hence, optimum pH for the DNA biosensor was occurred at pH 6.5 as it favoured the maximum rate of DNA hybridization reaction, which was indicated by the lowest AQMS oxidation response.

Generally, DNA hybridization reaction is more stable and rapid in high ionic strength solutions (i.e. cations such as Na^+ ion) as it could stabilize the configuration of dsDNA [2]. In this study, ionic strength of the DNA hybridization environment was altered by changing the NaCl concentration from 0.1–2.0 M and Na-phosphate buffer (pH 6.5) concentration from 0.01–0.50 M (Figure 5b and Figure 5c). When the ionic strength of the DNA hybridization medium was 0.05 M Na-phosphate buffer containing 0.5 M NaCl (pH 6.5), maximum DNA hybridization response was observed. This is attributed to the effect of neutralization of the negatively charged DNA sugar-phosphate backbone, thus reducing the electrostatic repulsion between DNA molecules and promoting DNA hybridization [1,22,23,24]. At other ionic strength and buffer conditions, DNA hybridization is not optimum and the absorption of aromatic AQMS on the basal plane of the immobilized rGO by π–π stacking could then occur.

3.5 DNA Immobilization Duration, DNA Hybridization Time and DNA Biosensor Long Term Stability Studies

The time required for the probes to fully occupy their immobilization sites on the poly(*n*BA-NAS)-rGO composite electrode is exhibited in Figure 6a. The AQMS DPV peak current decreased with time from 1–6 h as the number of DNA probe immobilized on the SPE increased with time. As a result, lesser and lesser AQMS molecules were able to adsorb on the electrode surface as time progressed. The AQMS DPV response achieved a plateau

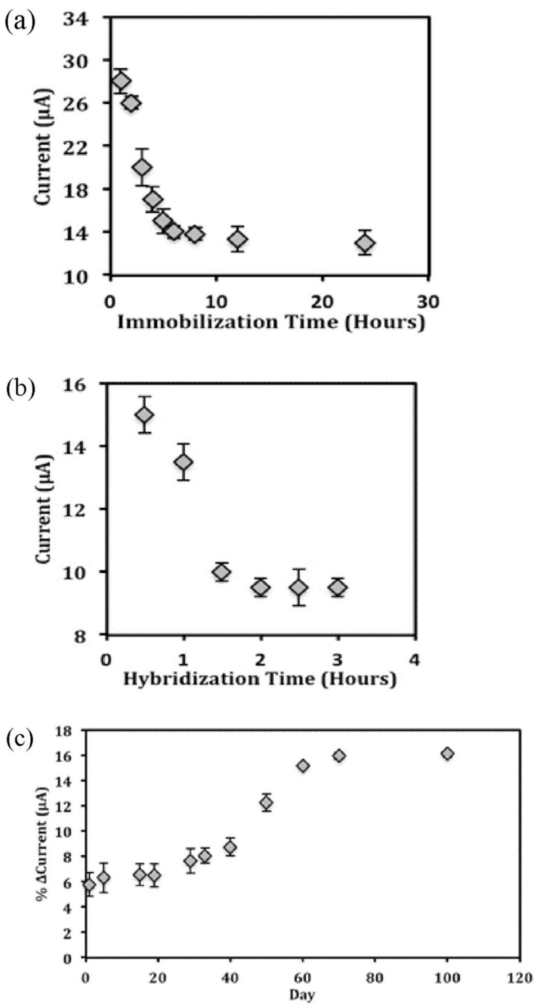

Fig. 6. DNA immobilization time (a), DNA hybridization duration (b) and shelf life (c) of the DNA biosensor studied in 5 μM target DNA using 1 mM AQMS in 0.05 M Na-phosphate buffer at pH 6.5.

response after 6 h of DNA probe immobilization duration, which indicated no further covalent attachment of aminated DNA probes onto the membrane. In a separate study, the time required for the DNA hybridization reaction to reach equilibrium was determined to be about one and a half hours (Figure 6b), whereby the AQMS DPV peak current became constant after 90 min of DNA hybridization time. However, the DNA hybridization time can be shortened by using electrokinetic methods including ion concentration polarization (ICP) [25] and isotachophoresis (ITP) [26] through surface-based DNA biosensor detection regime.

In terms of long term performance, the stability of the biosensor response in terms of change of DPV current (% ΔCurrent) from the initial response was shown in Figure 6c. For the first one month, the change of DPV current was low and the DNA biosensor was capable of retained 75% of its initial DPV response after one month of storage period. The DNA biosensor response was then slowly deteriorated from day −40 and onwards.

3.6 Dynamic Linear Range, Selectivity, Reproducibility and Practical Feasibility of The DNA Biosensor

Figure S3(a) in Supporting Information illustrates the DNA biosensor response towards various cDNA concentrations. The DNA biosensor DPV response at −0.5 V was found to decrease as the cDNA concentration increased. This was due to the immobilized dsDNA gradually building up a barrier with the increasing of the cDNA concentration, and hindering the access of redox active AQMS compound at the poly(*n*BA-NAS)-rGO composite electrode surface. This can be deduced that the target DNA quantification was based on the extent of AQMS adsorption, whereby the decrement of the AQMS DPV current was proportional to the increment of the amount of hybridized cDNA immobilized on the electrode surface. A linear DNA biosensor response was obtained in the range of 1.0×10^{-15}–1.0×10^{-8} M target DNA with a limit of detection (LOD) estimated at 6.3×10^{-16} M target DNA. The linear part of the plot of DNA biosensor DPV response versus logarithm of the target DNA concentration can be described by the regression equation, $y=-1.4928x+3.9647$ with a correlation coefficient, R^2 of 0.9966. The DNA biosensor also demonstrated satisfactory reproducibility performance using five individual DNA electrodes for DNA testing with two different cDNA concentrations [Figure S3(b) in Supporting Information]. The relative standard deviations (RSDs) for the reproducibility study were calculated at 3.7% and 4.6% for the detection of 1.0×10^{-5} μM and 1.0×10^{-8} μM cDNA, respectively.

The selectivity of the DNA biosensor towards CaMV 35S GM DNA was investigated with DNA mismatch assay via hybridization with different number of base mismatches in target DNA sequences, and compared with the result acquired with cDNA. The DNA biosensor showed a decreasing response trend with the reduction in the number of mismatch bases in cDNA sequences from 16-base to 2-base mismatched DNAs, and the lowest DPV peak current response was obtained with cDNA [Figure S3(c) in Supporting Information]. This is best explained by the fact that lower number of mismatch bases in the target sequences permitted higher degree of DNA hybridization reaction, and impeded the adsorption of AQMS at the electrode surface. This DNA detection mechanism was further confirmed by a control experiment with an electrode having immobilized poly(*n*BA-NAS)-rGO membrane without immobilised DNA probe where maximum AQMS response was obtained as a result of the maximum AQMS adsorption on the graphene-modified polyacrylic membrane of the electrode. The electrochemical DNA biosensor demonstrated recovery percentages within the range of 97.3–104.0% for a series of GM soybean DNA concentrations between 2.00×10^{-8} μg/mL and 5.00×10^{-4} μg/mL (Table 1). Thus, the DNA biosensor is useful for the assessment of GMO, particularly for GM food products.

Table 1. The recovery percentages of GM DNA found in GM soybean DNA extracts using the developed electrochemical DNA biosensor ($n=4$).

Sample	GM DNA concentration (certified) (μg/mL)	GM DNA concentration determined by DNA biosensor (μg/mL)	Recovery percentage (%)
1	2.00×10^{-8}	2.08×10^{-8}	104.0
2	4.00×10^{-7}	3.89×10^{-7}	97.3
3	5.00×10^{-6}	5.09×10^{-6}	101.8
4	6.20×10^{-5}	6.10×10^{-5}	98.4
5	5.00×10^{-4}	4.94×10^{-4}	98.8

3.7 Comparison of The Developed DNA Biosensor with Previously Reported GM Biosensors

The comparison of this DNA biosensor's performance with previously reported GM biosensors using different DNA carrier matrices and electrodes is summarized in Table 2. The analytical performance of the developed electrochemical DNA biosensor in this work demonstrated improved performance in terms of detection limit and dynamic linear range compared to other amperometric biosensors using DNA supporting materials like EDC (1-Ethyl-3-(3-dimethylaminopropyl)carbodiimide) and NHS (N-Hydroxysuccinimide) modified glassy carbon electrode (GCE) [27], platinum nanoparticles (PtNPs) modified GCE [28], mercaptoacetic acid modified Au electrode [29], single-walled carbon nanotube (SWCNT) and poly-L-lysine nanocomposite modified carbon paste electrode (CPE) [30] and polyacrylic microspheres-gold nanoparticles (AuNPs) composite modified SPE [31]. Besides, label-free electrochemical DNA biosensor using classic redox-active conductive polymers such as polyaniline and its graphene composite have also been employed

Table 2. The comparison of the analytical performance of the developed electrochemical DNA biosensor with other previously reported electrochemical GM biosensor using different biosensing materials.

Materials	Linear range (M)	LOD	Reproducibility	Ref.
Poly(nBA-NAS)-rGO modified SPE	1.0×10^{-15}–1.0×10^{-8}	6.3×10^{-16}	3.7–4.6% ($n=5$)	Present research
EDC and NHS modfied GCE	5.0×10^{-9}–1.2×10^{-7}	5.0×10^{-9}	-	[27]
PtNPs modified GCE	2.1×10^{-9}–2.1×10^{-7}	1.0×10^{-9}	5.9% ($n=5$)	[28]
Mercaptoacetic acid modified Au electrode	1.2×10^{-12}–4.8×10^{-8}	4.4×10^{-12}	–	[29]
SWCNT and poly-L-lysine modified CPE	1.0×10^{-12}–1.0×10^{-7}	3.1×10^{-13}	3.2% ($n=7$)	[30]
Poly(nBA-NAS)-AuNPs modified SPE	2.0×10^{-15}–2.0×10^{-9}	7.8×10^{-16}	2.7–4.7% ($n=5$)	[31]
DNA/polyaniline	1.0×10^{-10}–1.0×10^{-5}	1.0×10^{-10}	–	[32]
DNA/graphene/ polyaniline/GCE	1.0×10^{-13}–1.0×10^{-7}	3.1×10^{-14}	5.4% ($n=10$)	[33]

as redox active substrates to detect DNA hybridization [32,33] in order to eliminate the use of a separate redox reporter, and thus simplifies the sensor fabrication and detection processes. However, label-free detection of DNA could not be applied for low level DNA screening purposes, and this proved the redox active label is of paramount important in amplifying the hybridization signal and enhancing the sensitivity of the electrochemical label-based DNA biosensor.

4 Conclusions

The present work demonstrated a novel concept for specific detection of DNA by monitoring the adsorption of AQMS on the electrode surface, and DNA quantitation was performed by voltammetric analysis of AQMS redox electrochemistry. The graphene nanoparticles incorporated into the DNA biosensor platform played important roles in the biosensor function. It has not only allowed adsorption of AQMS but also imparted a good electrical conductivity to the membrane, thus allowing ultra-low detection limit at femtomolar levels for DNA at a broad dynamic range of the biosensor performance. The GM DNA biosensor also demonstrated possible rapid and simple DNA detection approach for practical food analysis of GM products.

Acknowledgements

We acknowledge financial support from the Ministry of Science, Technology and Innovation (MOSTI) for E-Science Fund (06-01-02-SF1242), National University of Malaysia (UKM) via research support from RACE2013/2015-023 and DPP-2016-064 and Ministry of Higher Education for MyBrain MyPhD scholarship for Raja Zaidatul Akhmar Raja Jamaluddin. We would like to thank the Malaysian Agricultural Research & Development Institute for providing the DNA materials for this study.

References

[1] F. R. R. Teles, L. P. Fonseca, *Talanta* **2008**, *77*, 606–623.
[2] F. Lucarelli, G. Marrazza, A. P. F. Turner, M. Mascini, *Biosens. Bioelectron.* **2004**, *19*, 515–530.
[3] R. Ziolkowski, L. Gorski, S. Oszwaldowski, E. Malinowski, *Anal. Bioanal. Chem.* **2012**, *402*, 2259–2266.
[4] M. Lipp, A. Bluth, F. Eyquem, L. Kruse, H. Schimmel, G. V. den Eede, E. Anklam, E. Anklam, *Eur. Food Res. Technol.* **2001**, *212*, 497–504.
[5] E. Palecek, M. Fojta, M. Tomschik, J. Wang, *Biosens. Bioelectron.* **1998**, *13*, 621–628
[6] Y. Sun, S. Wang, *Am. J. Biomed. Sci.* **2009**, *3*, 171–177.
[7] E. L. S. Wong, P. Erohkin, J. J. Gooding, *Electrochem. Commun.* **2004**, *6*, 648–654.
[8] Y. Xu, L. Zhao, H. Bai, W. Hong, C. Li, G. Shi, *J. Am. Chem. Soc.* **2009**, *131*, 5856.
[9] W. Yang, Y. Bai, Y. Li, C. Sun, *Anal. Bioanal. Chem.* **2005**, *382*, 44–50
[10] E. L. S. Wong, F. J. Mearns, J. J. Gooding, *Sens. Actuators B* **2005**, *111*, 515–521.
[11] E. L. S. Wong, J. J. Gooding, *Anal. Chem.* **2006**, *78*, 2138–2144.
[12] W. S. Hummers, R. E. Offeman, *J. Am. Chem. Soc.* **1958**, *80*, 1339–1339
[13] N. I. Kovtyukhova, P. J. Ollivier, B. R. Martin, T. E. Mallouk, S. A. Chizhik, E. V. Buzaneva, A. D. Gorchinskiy, *Chem. Mater.* **1999**, *11*, 771–778.
[14] S. Park, R. S. Ruoff, *Nat. Nanotechnol.* **2009**, *4*, 217–224.
[15] S. Stankovich, D. A. Dikin, G. H. B. Dommett, K. M. Kohlhaas, E. J. Zimney, E. A. Stac, R. D. Piner, S. T. Nguyen, R. S. Ruoff, *Nature* **2006**, *442*, 282.
[16] S. Perumbilavil, P. Sankar, T. P. Rose, R. Philip, *Appl. Phys. Lett.* **2015**, *107*, 051104.
[17] R. M. Zaid, F. C. Chong, E. Y. L. Teo, E. P. Ng, K. F. Chong, *Arab. J. Chem.* **2015**, *8*, 560.
[18] G. Yuan, G. Zhang, J. Chen, L. Fu, L. Xu, F. Yang, *J. Solid State Electrochem.* **2013**, *17*, 2711–2719.
[19] C. Batchelor-McAuley, Q. Li, S. M. Dapin, R. G. Compton, *J. Phys. Chem. B* **2010**, *114*, 4094–4100.
[20] J. Xu, Q. Chen, G. M. Swain, *Anal. Chem.* **1998**, *70*, 3146–3154
[21] L. J. Xiong, C. Batchelor-McAuley, L. M. Gon, J. A. Rodrigues, R. G. Comptona, *Biosens. Bioelectron.* **2011**, *26*, 4198–4203.
[22] Metzenberg. *Working with DNA*, Taylor & Francis. California State University Northridge, USA, **2007**.

[23] B. B. Hames, S. J. Higgins, *Nucleic Acid Hybridisation–A Practical Approach*, Oxford University Press, **1985**.
[24] D. Zhu, J. Liu, Y. Tang, D. Xing, *Sens. Actuators B* **2010**, *149*, 221–225.
[25] X. Wei, P. Panindre, Q. Zhang, Y. Song, *ACS Sens.* **2016**, *1*, 862–865.
[26] M. Bercovicia, C. M. Hana, J. C. Liao, J. G. Santiago, *Appl. Biol. Sci.* **2012**, *109*, 11127–11132.
[27] G. Xu, K. Jiaoa, J. Fanb, W. Suna, *Acta Chim. Slov.* **2006**, *53*, 486–491.
[28] X. Wang, S. M. Tabakman, H. Dai, *J. Am. Chem. Soc.* **2008**, *130*, 8152.
[29] W. Sun, J. Zhong, P. Qin, K. Jiao, *Anal. Biochem.* **2008**, *377*, 115–119.
[30] C. Jiang, T. Yang, K. Jiao, H. Gao, *Electrochim. Acta* **2008**, *53*, 2917–2924.
[31] A. Ulianas, Y. H. Lee, A. Musa, H. Lauc, I. Zamri, L. L. Tan, *Sens. Actuators B* **2014**, *190*, 694–701.
[32] Y. Zhou, B. Yu, A. Guiseppi-Elie, V. Sergeyev, K. Levon, *Biosens. Bioelectron.* **2009**, *24*, 3275–3280.
[33] M. Du, T. Yang, X. Li, K. Jiao, *Talanta* **2012**, *88*, 439–444.

Received: October 4, 2017
Accepted: November 27, 2017
Published online on ■■, ■■■

FULL PAPER